Journal of Magnetism and Magnetic Materials 465 (2018) 598–602

Contents lists available at ScienceDirect

Journal of Magnetism and Magnetic Materials

journal homepage: www.elsevier.com/locate/jmmm

Research articles

Effect of Bi-Co co-doping on the microstructure and magnetic properties of NiMgCuZn ferrites

Jiajia Pei, Zhi Wang*

School of Science, Tianjin University, Tianjin 300072, PR China

ARTICLE INFO

Keywords:
NiMgCuZn ferrite
Bi-Co co-doping
Soft magnetic properties
Magnetic losses
Initial permeability

ABSTRACT

$Ni_{0.15-x}Mg_{0.1}Cu_{0.3}Zn_{0.45}Bi_xCo_xFe_{2-x}O_4$ (x = 0, 0.01, 0.02, 0.03) ferrites were prepared by sol-gel auto-combustion method. The X-ray diffraction confirmed the formation of the single-phase spinel structure when $x \leq 0.02$. The microstructures were examined by SEM. The liquid phase produced by high temperature sintering promoted the grain growth and decreased the porosity. Magnetic measurements showed that saturation magnetization decreased continuously with the substitution of Bi and Co contents, whereas, the initial permeability increased with increase in Bi-Co content up to 0.02 followed by a decrease. In addition, Incorporation of Bi-Co resulted in the increase in quality factor and the decrease in loss factor, which implies that NiMgCuZn ferrite doped with Bi-Co is suitable for high frequency applications. Moreover, the $Ni_{0.13}Mg_{0.1}Cu_{0.3}Zn_{0.45}Bi_{0.02}Co_{0.02}Fe_{1.98}O_4$ sample exhibited the largest density, the highest initial permeability, and the lowest loss.

1. Introduction

The rapid development of electronic information technology has accelerated electronic devices towards to high frequency, high efficiency and miniaturization [1,2]. Soft magnetic ferrites as one of the nonmetallic magnetic materials are widely used in electronic communication and information storage devices on account of their excellent electrical and magnetic properties [3–5]. Wherein, NiMgCuZn [6] ferrites combine the merits of moderately high saturation magnetization and wide frequency applications of NiCuZn ferrites [7–9] and the cost effectiveness, high permeability of MgCuZn ferrites [10–13] which make them become good candidates for the further miniaturization of electronic devices.

Recently, many researchers have committed to improve the soft magnetic properties and reduce the losses at high frequency by doping ions to that ferrite system. It was reported that Co^{2+} substitution significantly reduced the core losses, which got a minimum around the compensation point of magnetocrystalline anisotropy [14]. Furthermore, the addition of moderate content of Bi^{3+} has been found to promote grain growth uniformly due to the formation of liquid phase on grain boundaries [15–17]. To sum up, although some literatures investigated the effects of the Bi^{3+} or Co^{2+} additive in NiMgCuZn ferrites, little attention has been concentrated on the Bi-Co co-doping. Thus, it is meaningful to achieve desired properties in NiMgCuZn ferrites by Bi-Co co-doping. In the present work, $Ni_{0.15-x}Mg_{0.1}Cu_{0.3}Zn_{0.45}Bi_xCo_xFe_{2-x}O_4$ (x = 0, 0.01, 0.02, 0.03) ferrites were prepared by sol-gel auto-combustion method, the microstructural and magnetic characteristics of sintered ferrites were also examined.

2. Experimental procedures

2.1. Preparation of materials

Bi-Co multi-doped Ni-Mg-Cu-Zn ferrite powders with nominal compositions of $Ni_{0.15-x}Mg_{0.1}Cu_{0.3}Zn_{0.45}Bi_xCo_xFe_{2-x}O_4$, where x varies from 0 to 0.03 in steps of 0.01, have been prepared by the sol-gel auto combustion method. The starting reagents used were analytical grade nickel nitrate [$Ni(NO_3)_2{\cdot}6H_2O$], magnesium nitrate [$Mg(NO_3)_2{\cdot}6H_2O$], copper nitrate [$Cu(NO_3)_2{\cdot}3H_2O$], zinc nitrate [$Zn(NO_3)_2{\cdot}6H_2O$], iron nitrate [$Fe(NO_3)_3{\cdot}9H_2O$], bismuth nitrate [$Bi(NO_3)_3{\cdot}5H_2O$], cobalt nitrate [$Co(NO_3)_2{\cdot}6H_2O$] and citric acid [$C_6H_8O_7{\cdot}H_2O$]. According to stoichiometric composition of $Ni_{0.15-x}Mg_{0.1}Cu_{0.3}Zn_{0.45}Bi_xCo_xFe_{2-x}O_4$, citric acid and metal nitrate were dissolved in deionized water, keeping the metal ion to citric acid ratio of 1:1 to form an aqueous solution. The pH of mixed solution was adjusted to 6 using ammonia. The solution was then heated up to 80 °C with continuously stirring to form a viscous liquid. The obtained sol was dried in an oven at 130 °C for about 24 h. The dried gel derived from metal nitrate and citric acid sol exhibited auto-combustion behavior. Once the dried gel was ignited at room temperature, it self-propagated until burnt out and obtained black, homogeneously dried powder. Then, a glass mortar and pestle was used to obtain a very fine powder after grinding. The fine powders were subsequently calcined at 600 °C for 2 h in

* Corresponding author.
E-mail address: zhiwang@tju.edu.cn (Z. Wang).

https://doi.org/10.1016/j.jmmm.2018.06.045
Received 22 November 2017; Received in revised form 10 June 2018; Accepted 16 June 2018
Available online 18 June 2018
0304-8853/ © 2018 Published by Elsevier B.V.

a muffle furnace for better crystallization and homogeneous cation distribution in the spinel. Finally, the synthesized powders were mixed with 10 wt% polyvinyl alcohol (PVA) solution and granulated. The granulated powders were uniaxially pressed at a pressure of 20 MPa for the toroidal specimens. The resulting specimens were sintered at 950 °C for 2 h with the heating rate 2 °C/min in air to form compact bulks and subsequently cooled to room temperature naturally in the furnace by overnight. These toroidal samples were used for structural and magnetic measurements.

2.2. Measurements

The crystal structure and the phase identification of the obtained samples were performed by X-ray diffraction (XRD, D8 Advanced, Germany Bruker) with Cu Kα radiation (λ = 1.5405 Å). The average crystallite size was determined by the full-width at half-maximum (FWHM) of the strongest diffraction peak (3 1 1) using the Scherrer formula. The morphologies of the sintered samples were observed using a Nanosem 430 field emission scanning electron microscopy (FESEM, America). The magnetization of the sintered ferrite was determined by a vibrating sample magnetometer (VSM, LDJ-9600, America). The experimental density of sintered ferrite was measured using the Archimedes principle. The initial permeability μ_i, was in situ measured in a furnace using HP4294A impedance analyzer at H = 0.4 A/m and f = 10 kHz. These measurements were carried out in the temperature range of 25–350 °C at 5 °C temperature intervals. Based on the temperature dependence of initial permeability (μ_i-T curve), the Curie temperature Tc can be determined. The loss factor (tanδ) and quality factor Q measurements of the resultant were carried out at 1 MHz using Magnetizing & Measuring Equipment.

The average crystallite size (D) of the sintered samples was calculated from X-ray peak broadening of the (3 1 1) peak with Scherrer's formula:

$$D = \frac{K\lambda}{\beta cos\theta} \quad (1)$$

where K is a constant, β is the full width half-maximum, λ is the wavelength of X-rays used and θ is the diffraction angle.

The lattice parameter (a) was calculated using the relation:

$$1/d^2 = (h^2 + k^2 + l^2)/a^2 \quad (2)$$

where a is the lattice parameter, (hkl) is the Miller indices and d is the interplanar distance.

Measured density ρ_b, X-ray density ρ_x and the porosity P are calculated according to the Eqs. (3), (4) and (5).

$$\rho_b = m/\pi r^2 h \quad (3)$$

where m was mass, r was radius and h was thickness of the pellet samples.

$$\rho_x = 8m/N_A a^3 \quad (4)$$

where M is the molecular weight of the sample, N_A is Avogadro's number and a is the lattice constant.

$$P = 1 - \rho_b/\rho_x \quad (5)$$

3. Results and discussion

Fig. 1 shows the XRD patterns of $Ni_{0.15-x}Mg_{0.1}Cu_{0.3}Zn_{0.45}Bi_xCo_xFe_{2-x}O_4$ (x = 0, 0.01, 0.02 and 0.03) bulk samples sintered at 950 °C. The XRD analysis confirmed the formation of single phase spinel structure when $x \le 0.02$, it is likely that Co^{2+} ions have entered into the crystalline lattice. Where for x = 0.03, there is a diffraction peak at 2θ = 28.3° and this impurity phase was identified as $Bi_{24}Fe_2O_{39}$ (JCPDS No. 65-3107). This may be attributed to the fact that the introduction of Co^{2+} could facilitate the formation of Fe^{3+} which caused the higher concentration of Bi^{3+} in grain boundary, thereby resulting in the formation of $Bi_{24}Fe_2O_{39}$ [15,18]. The

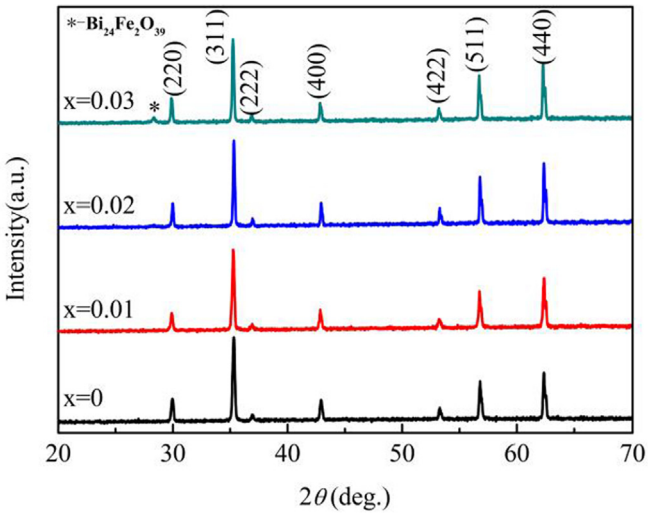

Fig. 1. X-ray diffraction patterns of $Ni_{0.15-x}Mg_{0.1}Cu_{0.3}Zn_{0.45}Bi_xCo_xFe_{2-x}O_4$ bulk samples sintered at 950 °C for 2 h.

average crystallite size (D) of the sintered samples was calculated from X-ray peak broadening of the (3 1 1) peak with Scherrer's formula. The results showed the crystallite sizes increase with the increase of Bi^{3+} and Co^{2+} especially for the sample of x = 0.03 as shown in Table 1. This can be accounted for the formation of liquid phase in the calcining process with the addition of Bi^{3+} ions, which increases the contact area of solid reaction and therefore accelerates the growth of the crystallite size [16,19]. Furthermore, the lattice parameter increased after the addition of small amount of Bi^{3+} and Co^{2+} ions ($x \le 0.02$) at first, which can be verified from the shift in peak position towards left, then dropped down when the doping amount of Bi^{3+} and Co^{2+} ions increased to x = 0.03. It is well known that the lattice parameter strongly depends on the difference between the substitution ion and host ion radii and the cationic distribution among the interstitial A and B sites of the spinel lattice [20]. The initial increase in lattice parameter of the as-prepared ferrite samples can be explained on the basis of the radii of metal ions in the samples. The radius of Co^{2+} ion (0.745 Å) is larger than that of Ni^{2+} ion (0.69 Å). So the replacement of Ni^{2+} in octahedral B sites by Co^{2+} would cause the expansion of unit cell, ultimately leading to the increase of lattice constant. However, the decrease of lattice constant with adding additional Bi^{3+} and Co^{2+} ions can be ascribable to the cation redistribution. The variation in lattice constant and crystallite size is shown graphically in Fig. 2 and individual values of all these parameters are listed in Table 1.

The data obtained from XRD was also utilized to determine X-ray density ρ_x, ρ_x was increased from 5.240 to 5.348 g/cm^3 with the incorporation of Bi and Co ions, which could be credited to the fact that the total molar mass of Co and Bi is larger than that of the Ni and Fe. The bulk density ρ_b exhibited an increasing behavior from 3.910 to 4.189 g/cm^3 when $x \le 0.02$. This in turn helped to determine the porosity P reducing from 25.38% to 20.81%. Whereas, for x = 0.03 ρ_b decreased to 4.141 g/cm^3 and P meanwhile increased to 22.57%, which is due to the abnormal growth of grain size. All these evaluated parameters are shown in Table 1.

Table 1
Lattice parameter (a), average crystallite size (D), bulk density (ρ_b), theory density (ρ_x), porosity (P) for $Ni_{0.15-x}Mg_{0.1}Cu_{0.3}Zn_{0.45}Bi_xCo_xFe_{2-x}O_4$ bulk samples.

x	a (Å)	D (nm)	ρ_b (g/cm^3)	ρ_x (g/cm^3)	P (%)
0	8.4190	33	3.910	5.240	25.38
0.01	8.4268	42	4.005	5.259	23.84
0.02	8.4288	54	4.189	5.290	20.81
0.03	8.4160	85	4.141	5.348	22.57

Download English Version:

https://daneshyari.com/en/article/8152826

Download Persian Version:

https://daneshyari.com/article/8152826

Daneshyari.com